Adherence of Phosphor Screens

S. Larach and J. E. McGowan
RCA Laboratories, Princeton, NJ 08540

Abstract—Properties of poly(vinyl alcohol), faceplate glass, phosphor slurries, and their interfaces have been investigated with respect to wet adherence of phosphor screens. Through measurements of bulk and interfacial properties, correlations of wet adherence were found with hydrodynamic parameters of PVA, using a new method of measuring adherence. The reasons for etching and precoating are discussed, and evidence is presented for a model involving glass surface silanol linkages to the PVA precoat, as well as the effects of the hitherto unsuspected glass-surface impurity layer due to etching. It has also been established for faceplate glass that each successive phosphor slurry sees a different surface in screening, the largest change being for the second phosphor deposited.

1. Introduction

While the PVA-dichromate system has been employed for many years in the world-wide production of color television picture tubes, there is a great paucity of data on the basic aspects of phosphor adherence to kinescope face-plates, a matter of great importance. The present study had three major aspects: (1) to determine the effect of various slurry additives on adherence, (2) to investigate basic screen adherence properties, in order to understand the processes that occur in screening and (3) to improve, if possible, the screen adherence of phosphors.

In defining the problem, we must also define the terms used. By *adherence,* we mean a phosphor screen, dot or line, or portion thereof, that is bonded to a glass substrate. This does not basically refer to particle-to-particle bonding, but rather the bonding of a particular geometric ensemble of phosphor particles to the glass

substrate and, in particular, to faceplate glass. In addition, we define *wet adherence* as the adherence of a phosphor screen after it has been wet with water, i.e., after development.

The experimental procedure for screening is shown in Fig. 1. The left portion of the figure involves the preparation of the substrate, faceplate glass (FPG); the right portion of the figure involves the chemical aspects of the phosphor slurry preparation/sensitization. The center portion of the figure treats of the screen application steps through developing, followed by wet adherence measurement by the jet impingement method. Although these steps are inter-related, different areas were studied by different techniques in order to arrive at a coherent model for phosphor screening.

Over the years, much practical lore has accumulated on phosphor screen adherence. Some beliefs are due to individual engineer's preferences or prejudices, but some constitute facts, more-or-less agreed to by the industry. These are usually based on invaluable experience in turning out a product, although the basic reasons for their use may have remained unknown. Two examples of these areas are etching of the substrate and use of a pre-coat prior to screening. These two particular aspects are part of the research reported here.

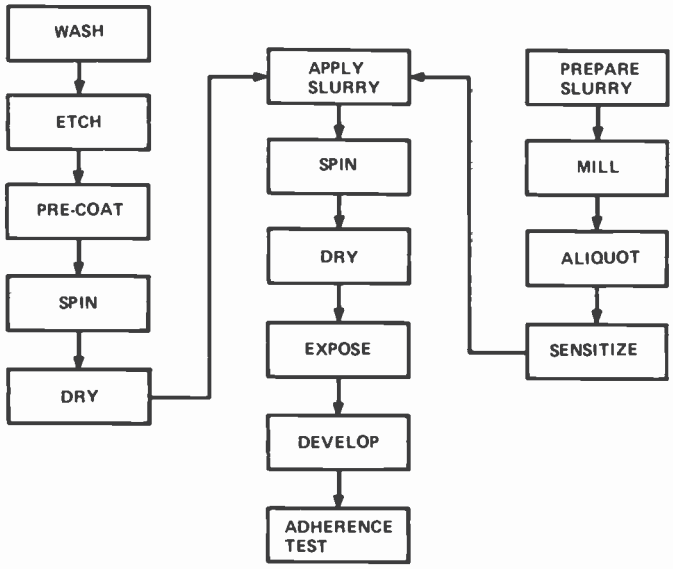

Fig. 1—Experimental procedure for screening.

In examining the overall problem of phosphor screen adherence, we decided to treat it as an interacting multi-interface system. As shown schematically in Fig. 2, we can consider a system comprising a section of faceplate glass (FPG) which forms interface I_1 and I_2, although some work was also done on the other interfaces. The way I_1 is affected by the etching treatment must also be considered in this analysis. The research involved the bulk properties of PVA, the FPG surface as affected by the etchant, the properties of dilute solutions of PVA, as used in precoats, and the surface chemistry of the glass. These will be treated in separate sections, as they relate to adherence.

The phosphor slurry was reduced eventually to its basic components: phosphor, PVA, water, and dichromate. This slurry is referred to as a model slurry in this paper. Phosphors were obtained from the RCA Video Components and Display Div., and the sensitizer was sodium dichromate. A variety of techniques were used in characterizing the various aspects of adherence.

This program was divided into several phases, the first of which was to evolve a method for studying adherence quantitatively. Adhesion measurements are best summarized by a statement from Mittal[1] in a 1981 paper: "Although there is available a cornucopia of adhesion measurement techniques, there is no single technique which can be recommended in all situations and which can be accepted by all those who have the need to measure adhesion. As a matter of fact, one should use that particular technique which best stimulates the usage conditions of the coating."

2. Adherence Measurements

To measure wet adherence of our screens, a zero-degree-spread jet

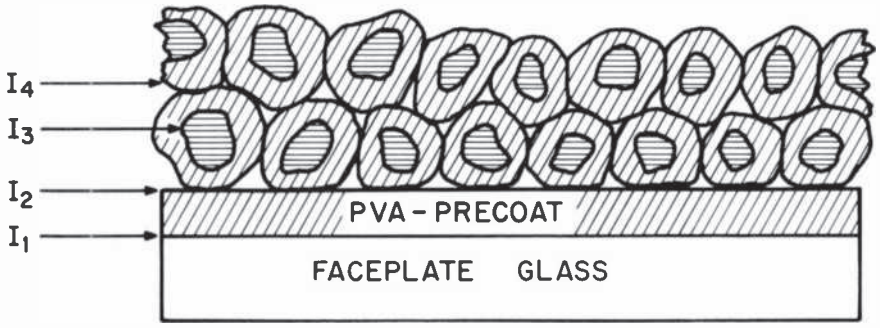

Fig. 2—Phosphor screen interfaces.

impingement method was evolved. In this method, a jet of de-ionized water, at a constant temperature, is impinged at constant pressure and time onto a wet screen that is a constant distance from the jet nozzle. The area of the screen lost is determined either by microscopic measurement or photometrically, and the wet adherence is taken as being inversely related to the area, i.e., the smaller the area of screen lost, the larger the adherence-factor. Relative adherence factor can then be plotted against some variable to compare the effects of changes or treatments.

An advantage of this method is that, with certain simplifying assumptions, values of "absolute" adherence can be calculated in ergs cm^{-2}. Both relative and absolute values of wet adherence are given in this paper. For a thorough treatment of the theory of particles in a water stream, the reader is referred to A. D. Zimon.[3]

Fig. 3 shows a typical plot for screen adherence, where the total jet kinetic energy is plotted against hole area for different times. The slope of the line yields a value of 8×10^7 ergs cm^{-2} for wet adherence for this particular case. Using a different and much more elaborate technique, Deryagin[2] has reported adherences of about 6

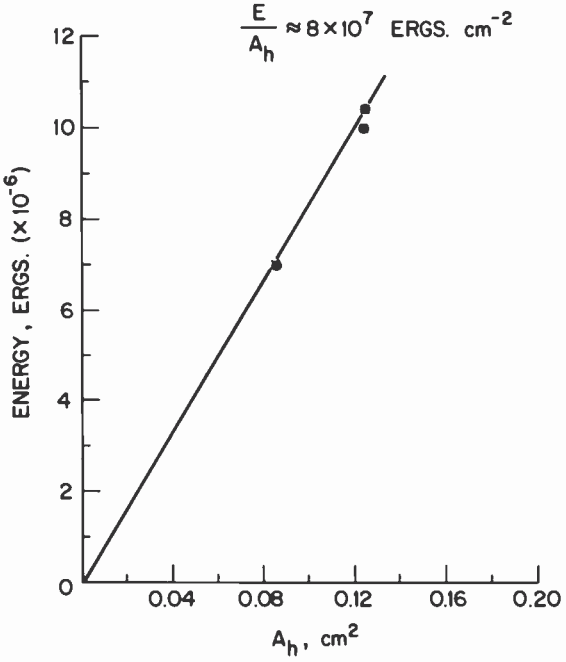

Fig. 3—Plot of kinetic energy vs hole area

$\times 10^5$ ergs cm^{-2} for polymer films on germanium surfaces, and about 3×10^4 ergs cm^{-2} for chlorinated PVC films on glass.

The mini-screening apparatus of Fonger[4] was adapted for use in our work (see Fig. 4). The holding tank for water was connected by ¼-inch stainless steel tubing to a pump capable of delivering water at 65 PSI at 21°C. The outlet side of the water pump was connected by ½-inch stainless steel tubing leading to a Jenkin's Bros. gate valve and an in-line valve reduction train. This consists of three Wilkerson brass reduction valves connected by ¼-inch stainless steel tubing to a Unijet zero-degree-spread nozzle, solid stream tip number 000019, 0.12 inch in diameter, obtainable from the Spraying Systems Co. Each Wilkerson reduction valve had a 0-60 PSI gauge attached to it.

To activate this system, the pump is turned on with a gauge pressure reading of zero. The Jenkins gate valve is opened, and by means of the speed control of the pump, the reading on the U.S. Gauge connected above the pump is raised slowly to 50 PSI. The first in-line Wilkerson reduction valve (nearest the pump) is set at 46; the next reduction valve is set at 40 PSI; and the last reduction valve before the solid stream nozzle is set at 36 PSI. The distance from the target is 7.8 cm. The target, a phosphor screen deposited on a 3×3 inch faceplate glass, is exposed and developed and set in an aluminum enclosure which is approximately a one foot cube, open at the top and at the jet-stream delivery side. The stream is permitted to hit the target for a given length of time. The target is dried under an IR lamp and the hole in the target is measured.

Nineteen-inch panels of virgin faceplate glass (FPG) cut into 3×3 inch sections were used in our experimental work. The glass sec-

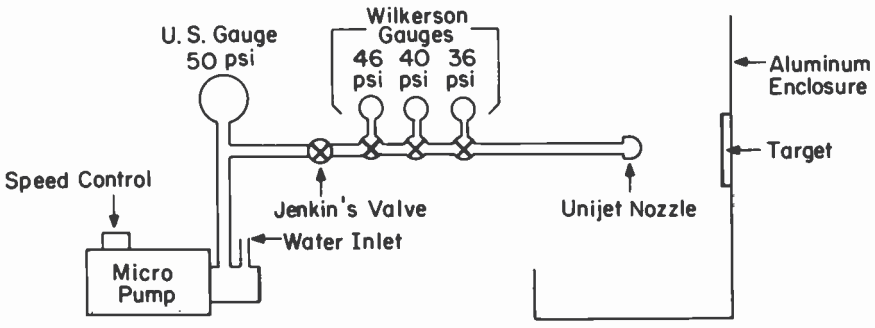

Fig. 4—Zero-degree-spread jet system for measuring adherence.

tions are first washed with a mild soap (Ivory) and warm tap water, followed by thorough rinsing in warm tap water and then in de-ionized water. The glass is then etched in a 5% solution of ammonium bifluoride for 30 seconds and rinsed with de-ionized water. While the glass is still wet, a precoat consisting of 0.5% poly(vinyl alcohol) at a pH of 2.7 is applied. This is done by using a Manostat syringe to apply the PVA uniformly over the glass surface. During PVA application, the glass rotates on a spinner at 7 rpm under a filtered 250 watt IR lamp 7 inches above the platform. As soon as the 2 ml of precoat PVA has been applied to the glass, the speed of rotation is increased to 96 rpm and the precoat is dried under the IR lamp for 5 minutes. Ten ml of phosphor slurry containing sodium dichromate is applied over the dry precoat on the faceplate glass at 7 rpm. The phosphor slurry consisted of the following formulation:

PVA 540/Total Solution = 3.5%
Phosphor/PVA = 12.5%
Pluronic/Phosphor = 0.1%
Phosphor/Total = 30%

After the phosphor slurry has been applied, the speed of rotation is increased to 96 rpm and the coating table holding the spinner is tilted to an angle of 105°. The IR lamp is attached to and tilts with the spinner, maintaining a constant normal incidence to the coating. The drying time is six minutes.

After the drying has ended, the spinner is tilted upright and the 3 × 3 inch glass section is removed. For the purpose of adherence testing, the entire phosphor coating is exposed using a bare 200 watt Hanovia X2-Hg compact-arc-lamp without a collimator. The source-to-coating distance is 13 inches, while the time of exposure can be varied.

After exposure, the coating is developed using 47°C deionized water for 30 seconds at 15 psi over a distance of 1 foot.

While still wet, the coating is set in the aluminum enclosure for adherence testing and is subjected to the jet stream. The coating is dried and the hole in the coating is measured for adherence calculation.

Fig. 5 shows wet adherence measurements for an RCA green-emitting phosphor, made into a model slurry, as a function of exposure time. We see, in this semi-log plot, the monotonic increase of adherence with exposure time until at about 55 seconds exposure, there is a sharp increase in adherence. Two reactions are proceeding; one at shorter exposure times with a specific rate constant of 4×10^{-4} sec^{-1} and a half-life of 1.7 msec, and one at larger

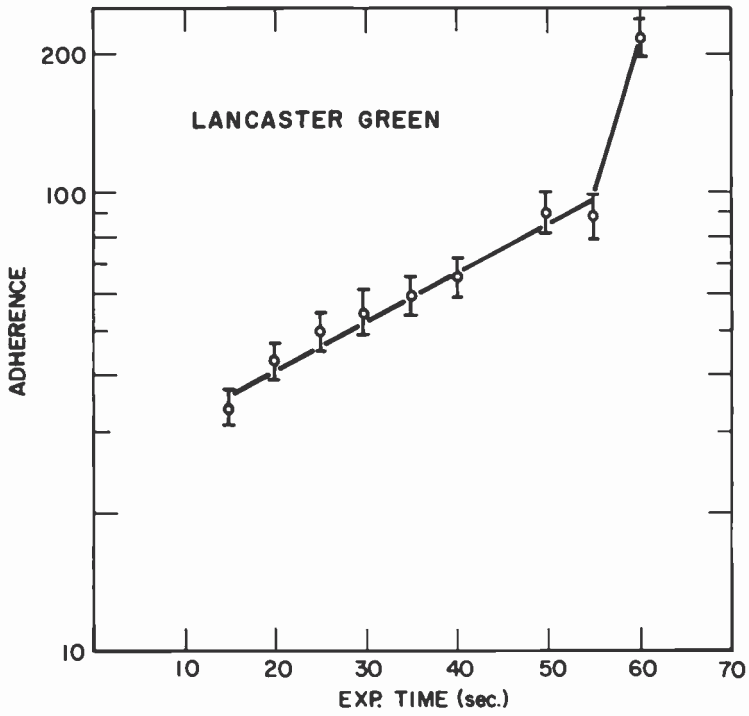

Fig. 5—Wet adherence vs exposure time.

exposure times with a specific rate constant of about 2.7×10^{-3} sec^{-1} and a half-life of about 25.6 msec.

3. Bulk PVA Properties

Poly(vinyl alcohol), PVA, is utilized in our manufacturing process both as a pre-coat and as a major part of the phosphor slurry, which is sensitized with dichromate. By poly(vinyl alcohol), we are referring to a material structured of linear molecules, A-$(CH_2OH)_p$-B, where p is the degree of polymerization and the end groups A and B are small and chemically inert. The average sterochemistry of the vinyl groups with respect to each other determine the *tacticity*. However, PVA, usually prepared from poly(vinyl acetate), may have minor structural complications because of side reactions. These are summarized in Table 1.[10] While PVA easily loses water when heated at 60°–100°C, this does not provide complete dehydration. Complete dehydration of PVA has been reported[11] by exposure for at least five hours to a suspension of calcium hydride in dry

Table 1—Main Structural Deviations from $-(CH_2CHOH)_p-$ Contained in Poly(vinyl alcohol) (From Pritchard[10])

Structure	Likely percent of monomer units	Cause
$-CH(OR)CH_2-$	0–5% (ethers)	Chemically incomplete reaction during transformation to PVA
$-CH(OCOR')CH_2-$	0–5% (ethers)	
$-CH_2CHOHCHOH-CH_2CH_2CHOH-$	0–2%, vinyl esters 0–1/2%, vinyl ethers	Occasional condensation of monomer by α-carbon
$-CH_2COH(CH_2CH_2-OH-)CH_2CHOH-$	0–0.05%	Elimination of hydrogen atoms at α- and β-carbon to start branches
$-CH(CH_2CHOH-)-CHOH-$	0–0.05%	
$-CH_2COH(CH_2CHOH\ CH_2CH_2OH)-$	Not easily estimated	Termination of chain end by abstraction of hydrogen on penultimate α-carbon
$-CH_2(C=O)-$	0–0.02%	Oxidation by air, especially catalyzed by bases
Cyclic ketal in single chains, and ketal between two chains	Very small	Condensation of oxo and hydroxy groups
Ether formation in single chains, and cyclic ether in single chains	Very small	Dehydration
$-CH=CH-$	High if polymer heated in right medium	Dehydration
$-CH_2OH$ end group	(Ideal)	Termination of propagating chain by abstraction of hydrogen atom
$-CH(OH)X$ end group	0–50%	Termination by X
$-CHO$ end group	0–50%	Elimination of catalyst residue as HX, from end group; especially HX = RCO_2H, ROH, or H_2O
Interchain cyclic acetal	Not easily estimated	Condensation of aldehyde group at end of chain with hydroxy groups

pyridine at 117°C. The resultant dehydrated product was a black polymer containing long chains of CH = CH groups. To examine some of the basic properties of PVA, particularly in dilute solutions (the PVA concentration in precoats is about 0.5% or less), measurements of viscosity were carried out.

3.1 Viscosity

If force per unit area, s, causes a layer of liquid at a distance x from a wall to move with a velocity, v, the viscosity, η, is defined as the

ratio between the shear stress s and the velocity gradient $\partial v/\partial x$ or rate of shear, γ, so that

$$S = \eta \frac{\partial v}{\partial x} = \eta\dot{\gamma}. \quad [1]$$

A very convenient way of characterizing PVA materials is by their viscosities. In our work, we used an Ubbelohde viscometer, in a thermostatted water bath held at 30°C. The initial PVA solution was less than 1% and was diluted after each run to the desired concentration. Thermal equilibrium times were taken into account throughout the experiments, and triple-distilled water was used as a reference standard before each measurement.

Specific viscosities, η_{sp}, were obtained from flow-time measurements for water and for the PVA solutions. The intrinsic viscosity, $[\eta]$, is defined* as

$$[\eta] = \lim_{c \to 0} (\eta_{sp}/c), \quad [2]$$

where c is the PVA concentration in grams per deciliter. $[\eta]$ was obtained by extrapolating the reduced viscosity, (η_{sp}/c) plotted against c, to zero concentration. Fig. 6 illustrates our results for three different PVA materials.

Intrinsic viscosities characterize polymers where the individual polymer molecules can be taken as being essentially free of the influence of neighboring molecules. Again, this is of particular interest for PVA precoats, since dilute solutions are involved. We can compare our intrinsic viscosities with the intrinsic-viscosity-molecular-weight relationships reported for aqueous solutions of PVA. Using the equation of Matsumoto and Ohyanagi[5],

$$[\eta]_{30°C} = 4.25 \times 10^{-4} \overline{M}_w^{0.64} \quad [3]$$

we obtain $[\eta] = 1.7$ for PVA540, compared to our 1.08, which is in good agreement considering our nonfractioned PVA.

Elias[6], in a review of available data, has published the equation

$$[\eta]_{25°C} = 7.31 \times 10^{-4} \overline{M}_w^{0.616} \quad [4]$$

found to apply over a range of PVA molecular weights from 10^4 to 5×10^5. Using the Elias equation, we obtain $[\eta]_{25°C} = 0.97$ for our PVA540 material, again as against our $[\eta] = 1.08$ value, at 30°C.

* Note that $[\eta]$ is given in deciliters per gram, and is sometimes referred to as the "limiting viscosity number" in the revised clasification system recommended by IUPAC in 1952.

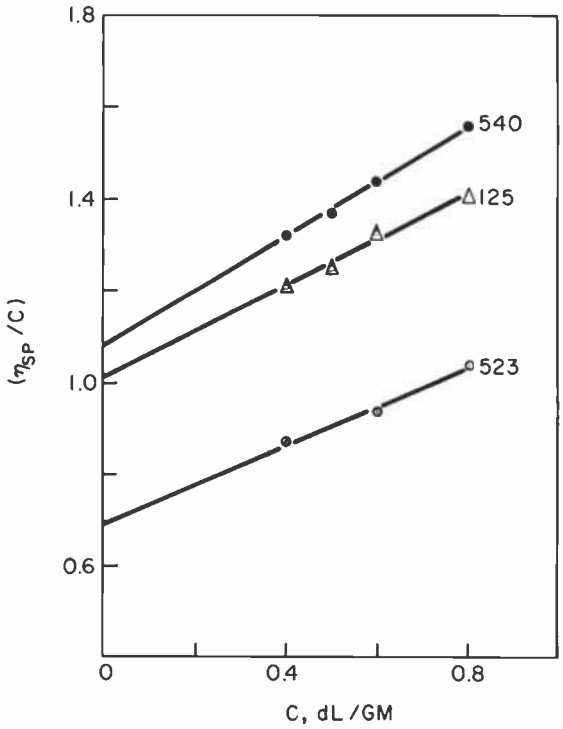

Fig. 6—Reduced viscosity vs concentration of PVA.

The effect of temperature on the intrinsic viscosity of PVA in water has been given by Sakurada[7] as

$$[\eta]_T = 1.07^{-(T-20)/10}[\eta]_{20°C} \quad [5]$$

It should be noted that the Elias equation is of the form $[\eta] = KM_w^a$, in which K and a are constants, usually independent of molecular weight but dependent on the nature of the polymer. This type of equation is usually referred to as the Mark-Houwink equation, and is applied to fractionated polymers or to polymers with narrow molecular weight distributions.

3.2 Basic Hydrodynamic Parameters

Flory[8] has evolved a hydrodynamic equation for the intrinsic viscosity of long-chain molecules in solution. In its simplified form,

Table 2—Hydrodynamic Parameters of Selected Samples of Poly(vinyl alcohol)[a]

PVA Type	Degree of Polym.	Degree of Hydration	$<r_o^2>^{1/2}$	$<s^2>^{1/2}$	R_h[b]	$[\eta]_{expt}$
540	2400	0.88	393Å	160Å	96Å	1.08
125	1800	0.996	336	137	82.	1.02
523	1800	0.88	307	125	75	0.69

[a] appropriate corrections in molecular weight made for residual acetyl groups.
[b] ζ is taken as 0.6 for the calculation of R_h. See Garvey, Tadros, and Wilson, *J. Colloid of Interface Sci.* 49 (1), 64 (1974).

this equation states that

$$[\eta] = \Phi \left(\frac{\overline{r_o^2}}{\overline{M}} \right)^{3/2} \overline{M}^{1/2}, \qquad [6]$$

where Φ is a fundamental constant, which for linear vinyl polymers is 2.1×10^{21}; $\overline{M}$ is the molecular weight, and $<r_o^2>$ is the mean square end-to-end distance of the unperturbed polymer chain. Thus, $(r_o^2)^{1/2}$ constitutes the root-mean-square end-to-end distance. Other basic hydrodynamic parameters* include $<s^2>^{1/2}$ radius of gyration, or the rms distance of the elements of the chain from its center of gravity, and R_h, the hydrodynamic radius.

The hydrodynamic parameters were calculated for PVA Samples 540, 125 and 523, and are given in Table 2.

It is interesting to compare our results for PVA 540, the material presently in use, to published values of other, similar, materials. Thus, Koopal and Lyklema[9] worked with Wacker (FRG)PVA of 0.88 degree of hydrolysis and molecular weight similar to our PVA 540. Their chain dimension parameters for this material are 380 Å for the end-to-end distance, and 160 Å for the radius of gyration, both in excellent agreement with our findings. As a check, the viscosity characteristic of PVA 540 at several concentrations were determined with a Ferranti direct-reading viscometer at various shear rates. The viscometer was first calibrated against NBS viscosity standards. Experimental values were converted to specific viscosities, which were then corrected to zero shear rate by extrapolation. Plots of corrected viscosities against concentration gave a value of 1.1 for the intrinsic viscosity of PVA 540, as against 1.08 determined by the generally accepted Ubbelohde method.

* See, for example, F. W. Bilmayer, Textbook of Polymer Science, Interscience, NY, 1964.

3.3 Rheology of Phosphor Slurry

We have investigated the rheology of our green phosphor model slurry, using a Ferranti-Couette viscometer, which has the advantage of being able to operate at varous shear rates, which is ideal for this examination. We found the viscosity of both resist and slurry to be Newtonian, i.e., following Eq. [1]. Results are shown in Fig. 7, with shear rate (sec^{-1}) plotted against shear force (dynes cm^{-2}). There was no evidence of thixotropy.

4. Pre-coat Properties

The role of the PVA pre-coat (PC) in screening has been a puzzling one for many years, although the necessity of a PC seems to have been well established. In our experiments with faceplate glass, we found the PC to be essential to good adherence. We therefore investigated some of the properties of the PC layer as they relate to adherence.

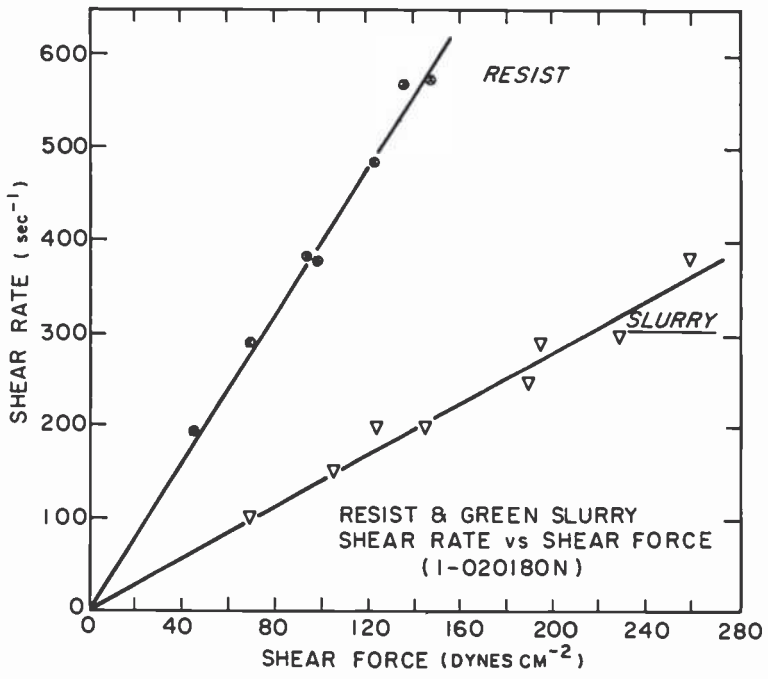

Fig. 7—Shear rate vs shear force for resist and green slurry.

4.1 Adherence and Pre-Coat Hydrodynamic Parameters

While it is difficult to correlate adherence with "normal" PVA pre-coat parameters, such as degree of polymerization and degree of hydrolysis, an excellent correlation is arrived at with hydrodynamic parameters. Fig. 8 is a plot of relative wet adherence against the hydrodynamic parameters derived in Table 1. We see that wet adherence increases with increasing hydrodynamic radius, radius of gyration, and the rms end-to-end distance of the unperturbed polymer chain. Thus, from Fig. 8, PVA 540 used as a pre-coat yields a phosphor screen with ten times greater wet adherence than PVA 523 and about 50% greater than PVA 125. It is of interest that in going from a degree of hydrolysis (DH) of 88% for PVA 523 to a DH of 99.6% for the PVA 125, both with the same degree of polymerization, the wet adherence increases seven-fold. It is apparent therefore that the hydrodynamic parameters of the PVA pre-coat are of

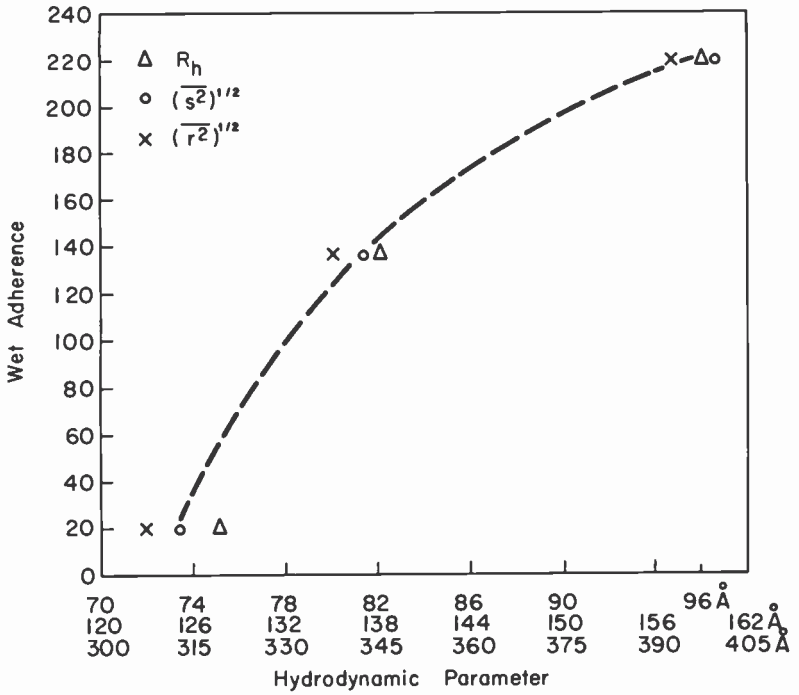

Fig. 8—Relative wet adherence vs hydrodynamic parameters.

great importance in determining the wet adherence of the phosphor screen.

4.2 Tacticity

Natta[12] devised the nomenclature which describes stereoregular configurations involving an asymmetric carbon. The *isotactic* configuration results when all the substituent groups R are above or below the plane of the main chain. If the R-groups lie alternately above and below the plane, the configuration is *syndiotactic,* and if the R-positions are random, the configuration is *atactic* or *heterotactic*. Fig. 9, from Finch[13], shows an example for PVA, where the polymer chain is shown in the fully-extended planar position.

Infrared spectra are used frequently to measure tacticity, and we have determined the tacticities for several of our PVA samples. Table 3, from Pritchard[10], after Liang and Learson[14], lists some characteristics of the IR spectrum of PVA. The bonds occurring at 916 cm^{-1} and at 850 cm^{-1} are characteristic skeletal vibrations of syndiotactic and isotactic PVA, and the percent tacticity is often arrived at from empirical relationships between tacticity and the ratios of the optical densities at these cited frequencies. For example, Kennedy and Willcockson[15] give:

$$\text{Percent syndiotactic} = 60\,(D_{916}/D_{850}) + 7 \qquad [7]$$

$$\text{Percent isotactic} = 59\text{–}78\,(D_{916}/D_{850}) \qquad [8]$$

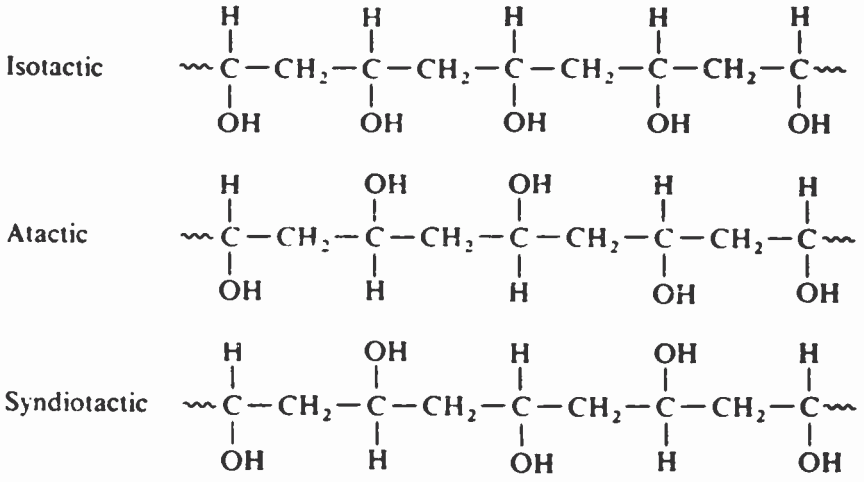

Fig. 9—Tacticity of PVA.

Table 3—Characteristics of the Infrared Spectrum of Poly(vinyl alcohol)[10,14]

Frequency (cm^{-1})	Relative intensity	Likely assignment
3340	Very strong	O—H stretching
2942	Strong	C—H stretching
2910	Strong	C—H stretching
2840	Shoulder	C—H stretching
1446	Strong	O—H and C—H bending
1430	Strong	CH2 bending
1376	Weak	CH2 wagging
1376	Medium	C—H and O—H bending
1320	Weak	C—H bending
1235	Weak	C—H wagging
1215	Very weak	
1144	Medium	C—C and C—O stretching
1096	Strong	C-O stretch & O-H bend
1087	Shoulder	
1040	Shoulder	
916	Medium	Skeletal
890	Very weak	
850	Medium	Skeletal
825	Shoulder	CH2 rocking
640	Medium, very broad	O—H twisting
610	Weak	
480	Weak	
410	Weak	
360	Shoulder	
185	Very weak	
135	Very weak	

Table 4 lists the tacticities and carbonyl for several of our PVA samples. It should be noted that (1) the sum of the tacticities is not exactly 100% due to the formulae utilized; and (2) the tacticities of the presently used pre-coat, PVA 540, are not greatly different from those of PVA 125 and PVA 523. Differences are found in syndiotactic and isotactic content compared to PVA 425. It is interesting that PVA 125, nearly 100% hydrolyzed, showed no detectable carbonyl; PVA 425 (about 96% DH) had 0.8% carbonyl; while PVA 523 and PVA 540 each 88% DH), had about 4% carbonyl. Carbonyl content varies inversely with DH.

Table 4—Tacticities and Carbonyl for Several PVA Samples

PVA	D.H.	Syndiotacticity	ISO.	Hetero.	Carbonyl
125	99.6%	25%	36%	40%	0
425	95.5%	20%	42%	38%	0.8
523	88%	25%	36%	40%	4.0
540	88%	25%	37%	38%	3.7

4.3 Pre-Coat Hydroxyl Content

Results obtained on PVA powders, using FT-IR, 100 scans, showed a relationship between wet adherence and the hydroxyl concentration of the pre-coat PVA. This is shown in Fig. 10 for green phosphor model-slurry where three different pre-coats were used, all at 0.5% concentration and all at pH 2.7. These results corroborate the findings that for this PVA group of low (79,000) molecular weight, wet adherence was found to increase with increasing degree of hydrolysis. It should be noted, however, that the molecular weight of the PVA appears to have an over-riding effect on wet adherence. Thus, the 88%-hydrolyzed PVA 540 showed a wet adherence nearly an order greater than the corresponding low molecular weight PVA. Again, the important aspects are the hydrodynamic parameters.

It is interesting to compare the hydroxyl concentration results with those for wet adherence as a function of degree of hydrolysis, as shown in Fig. 11, for 0.3% PVA. We see, as expected, the sharp dependence of wet adherence with degree of hydrolysis for these three samples of PVA. Note that the lowest adherence, 22 in^{-2}, is

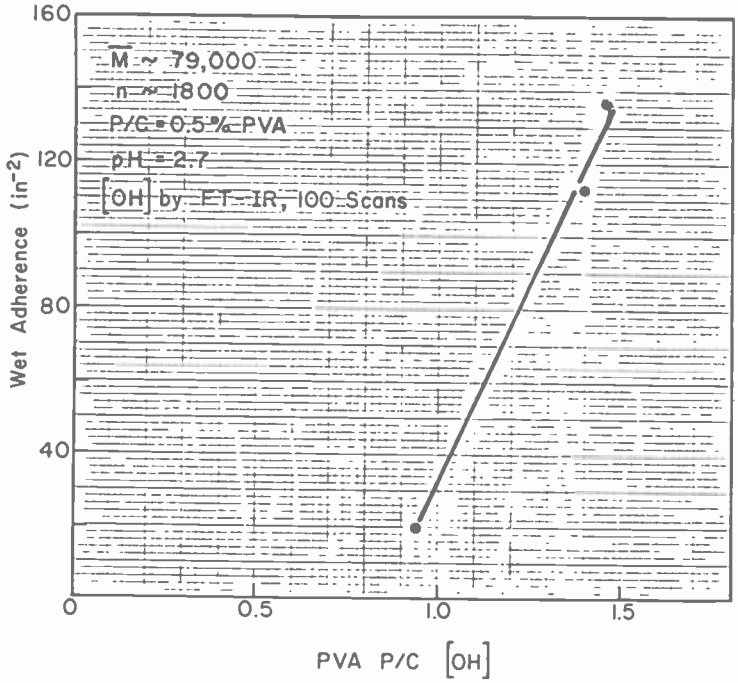

Fig. 10—Wet adherence vs pre-coat hydroxyl concentration.

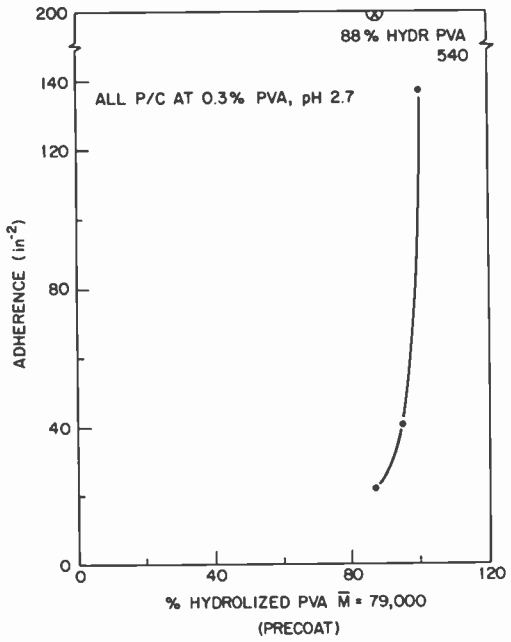

Fig. 11—Wet adherence vs degree of hydrolysis of PC-PVA.

for PVA 523 with DH = 0.88 and DP = 1800. For PVA 540, with DH = 0.88, but with DP = 2400, the adherence was about 200 in^{-2}, as indicated at the top of the figure.

4.4 Adherence and Pre-Coat pH

Wet adherence has been found by Harper[16] and by Wilcox[17] to be affected by pH. This effect was corroborated here, and was also found to depend on the type of glass substrate. Samples of model slurry were prepared, and the wet adherence was checked for 0.5% PVA at various pH's, using FPG or soda lime glass (SLG) substrates.

It is seen from Fig. 12 that wet adherence for FPG substrates increases with decreasing pre-coat pH, the effect leveling-off as pH = 1 is reached. The screen *quality* is poorer at the very low pH pre-coats, however, and we chose pH = 2.7 for our pre-coat work. The adherence of 4 screens made on SLG shows better adherence than those on FPG; adherence levels off at a pH of about 3.7 and remains constant to at least pH = 1.5. Other differences due to glass type will be described in the section on glasses.

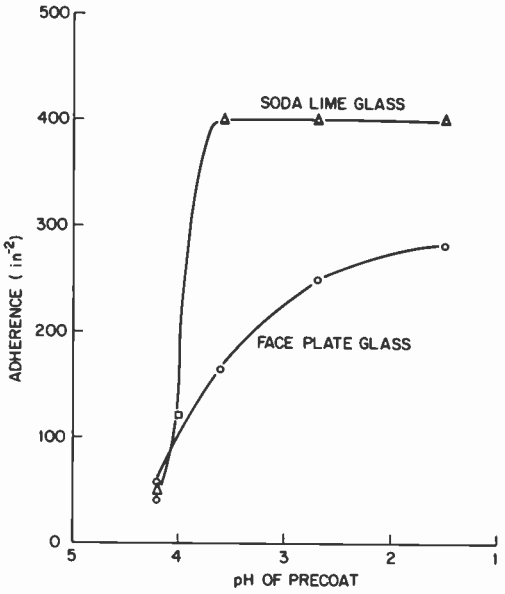

Fig. 12—Wet adherence vs pre-coat pH.

4.5 Pre-Coat Thickness Effects

A series of screens was prepared where the pre-coat thickness was varied by using PVA solutions of different concentrations, all at pH 2.7. Tallysurf measurements[18] were made of the PVA pre-coat thickness, and a plot of PVA concentrations versus PC thickness is shown in Fig. 13 for 0–4% PVA. The relative adherence plotted against PVA pre-coat thickness, for thicknesses from 0.18 μm to about 1.5 μm is shown in Fig. 14A. There is a striking decrease in adherence in going from 1800 Å to 2000 Å, followed by a constant adherence to at least 1.5 μm thickness of pre-coat. Further investigations of even lower concentrations of pre-coat PVA yielded results shown in Fig. 14B. Here, we have plots of wet adherence versus percent PVA concentration in the PC for SLG and FPG. The optimum PVA concentration was about 0.3%, which, for FPG, yielded a PC thickness of about 600 Å. Thickness points of 400 Å and 1000 Å are also indicated. Again, the SLG substrates show greater adherence. Knowing the area, density of solid PVA, and the volume (0.08 nm^3) and the cross-sectional area of a PVA segment (0.2 nm^2) from the work of Koopal and Lyklema[9], it can be calculated that the optimum pre-coat thickness consisted of about 200

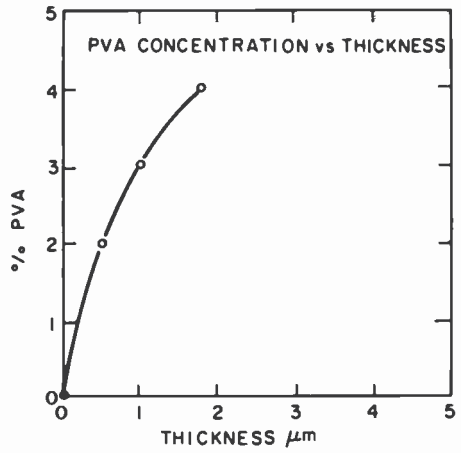

Fig. 13—PVA concentration vs PC thickness.

monolayers. Our work also indicated a retention of 3.9% for PVA pre-coat after spin-off. Apparently, there is an optimum pre-coat thickness for maximum adherence, again involving interfaces 1 and 2. Yakhinin[20] has reported that forming an adsorbed layer of PVA

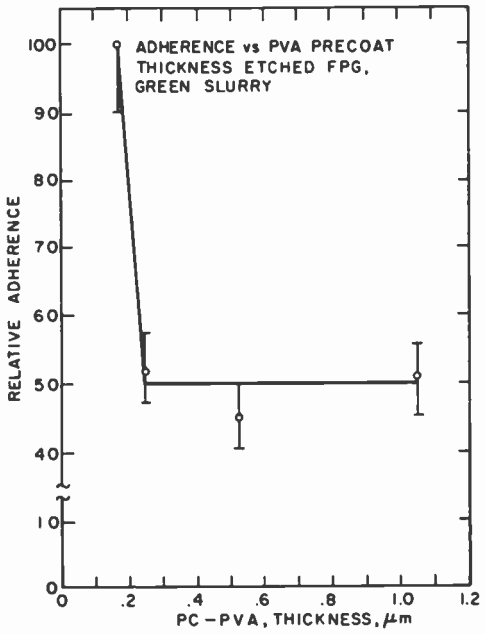

Fig. 14A—Relative adherence vs PC thickness.

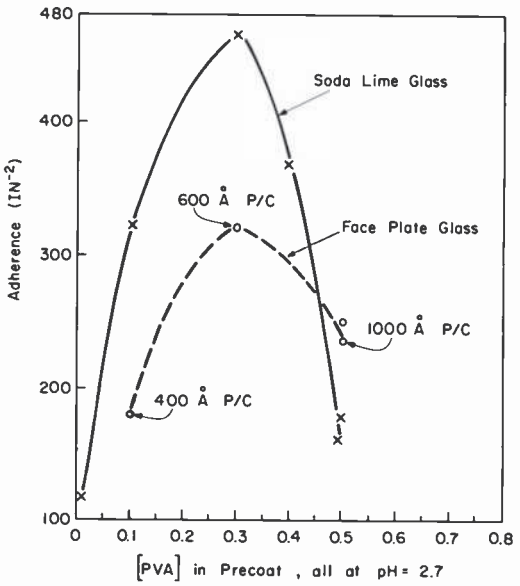

Fig. 14B—Wet adherence vs pre-coat PVA concentration.

decreased the contact interaction between a glass plate and 45 μm particles of rutile.

4.6 ζ-Potential

A potential difference exists between the surface of a particle and the bulk solution because of a charge density localized in the plane of its surface. Since the system as a whole is electrically neutral, this surface charge is balanced by an opposite equal excess ionic charge in the liquid phase that will concentrate in the vicinity of the particle surface.

When such a system is put in an electric field, the particles move toward the oppositely charged electrode, the counter ions moving in the reverse direction. The particle velocity increases with the ζ-potential of the particle. Thus, by using an electrophoretic mobility apparatus, we can derive ζ-potentials.

The greater the ζ-potential of a particle, the greater the repulsive force between it and similar particles. If two such high ζ particles are driven together thermally or mechanically, they will tend to separate in spite of van der Waal's forces tending to bind them

together. This could conceivably be of importance in such screening characteristics as porosity, line definition and cross-contamination.

The Micromeritics Model 1202 Electrophoretic Mass Transport Analyzer is capable of measurements under very high solids loading conditions. With this instrument, we determine the average particle electrophoretic mobility:

$$V_\epsilon = \frac{\Delta W \lambda}{ti\,\phi(1 - \phi)(\rho_p - \rho_L)}, \qquad [9]$$

where V_ϵ is the mobility, ΔW is the mass difference, i is the current, t the time, λ the specific conductance, ϕ the volume fraction of dispersed matter, and ρ is the density of the particle (p), or of the liquid (L).

The zeta-potential is then calculated from the Smoluchowski equation relating ζ to electrophoretic mobility, viscosity η, and dielectric constant D_t:

$$\zeta = \sigma\left(\frac{4\pi\eta}{D_t}\right) \qquad [10]$$

or, in the case of our instrument,

$$\zeta = \frac{4\pi(\Delta W)\lambda\eta}{ti\,\phi\,(\rho_p - \rho_L)D_T}. \qquad [11]$$

Since our 3 × 3 inch FPG slides could not be accommodated in the apparatus, faceplate glass was crushed and ground to a powder. Blank FPG had $\zeta = +4$ to $+6$ mV. However, FPG which had been etched (5% NH_4F) and washed had $\zeta = +130$ mV, while etched, washed, and PVA-coated FPG had $\zeta = +73$ mV. This was the first indication that the adsorbed ions due to etching of the glass imparted a highly positive zeta-potential to the FPG, which is reduced but remains highly positive after adsorption of small amounts of PVA from the 0.5% pre-coat. Fig. 15 illustrates the effect on the zeta-potential of increasing amounts of PVA. While this particular curve was obtained for pre-pigmented red-emitting phosphor, similar results were obtained with green. This Y919F Fe_2O_3-coated red phosphor has a specific surface area of 0.350 m^2gm^{-1}; the total phosphor area was 15.75 m^2.

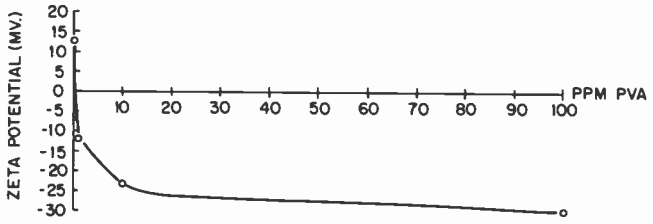

Fig. 15—Zeta potential vs PVA concentration.

Tadros[21] has published on the variation of zeta-potential with concentration of PVA adsorbed on an organic substrate and has obtained similar shapes, which he explains by invoking the macromolecules having a flat configuration which leads to thicker adsorbed layers. This will cause a shift in the shear plane toward the solution, leading to a lowering of zeta-potential until it reaches a limiting value.

Koopal and Lyklema[9] investigated the adsorption of PVA on silver iodide by double layer measurements using PVA samples similar to PVA 540. They report that the first 0.15 mg/m^2 adsorb in trains or flat loops; PVA in excess of this amount is adsorbed as loops. A detailed analysis of this first layer found there were twice as many trains as loops.

Garvey et al.[23] have compared different adsorbed layer thicknesses of PVA on polystyrene latex particles. For a 0.87 hydrolyzed PVA (M_w = 67,000, $<\bar{S}^2>$ = 117 Å, R_h = 67.5 Å), they report an effective thickness of the adsorbed PVA layer of 380 + 50 Å. It is interesting to compare this value for a PVA with small hydrodynamic factors and molecular weight with our value of 600 Å for the optimum PVA pre-coat thickness for adherence.

4.7 Adsorbed PVA

Examination of the green phosphor slurried in PVA showed, by the boric acid-iodine method of Zwick[19], that PVA *is* adsorbed onto the phosphor particles. This analytical method, highly sensitive for small amounts of PVA, was extended to larger amounts. A typical calibration curve is shown as Fig. 16, and Fig. 17 shows an adsorption curve for PVA in pre-pigmented red-emitting phosphor; axes are given in γ-PVA per millimole Y_2O_2S:Eu, and γ-PVA per square

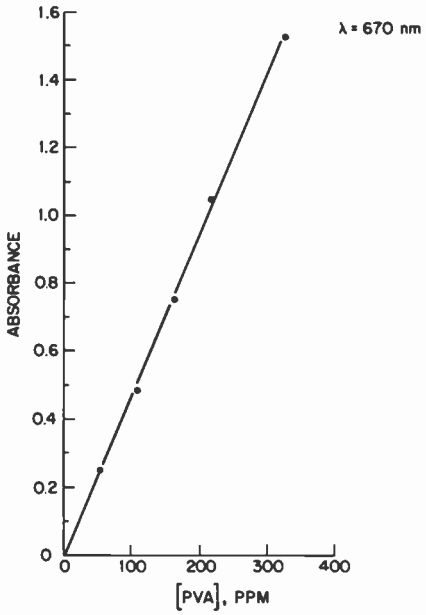

Fig. 16—Calibration curve for PVA adsorption.

meter surface area of phosphor. Similar results were obtained for green phosphor.

While one may speculate about a negative-ζ particle coated with PVA impinging on a positive-ζ FPG substrate to provide initial sticking, our measurements indicate that the FPG is even more positive *without* the pre-coat. However, our adherence tests show adherence failure without the pre-coat. Zeta-potentials by themselves, therefore, do not provide a complete explanation, but do constitute an important aspect of adherence, particularly with respect to the FPG.

In polymers and in glass, adhesion is believed to involve functional groups with large group dipole moments.[2] One could then have good adherence due to the asymmetrical electron density distribution in the contact zone, leading to an electrical-double-layer. Table 5 gives some pertinent values for several materials.

In the reactions of organic molecules with the molecules of a substrate, the major factors are the electronic processes that occur in the molecules and in the contact zone. If an asymmetric electron

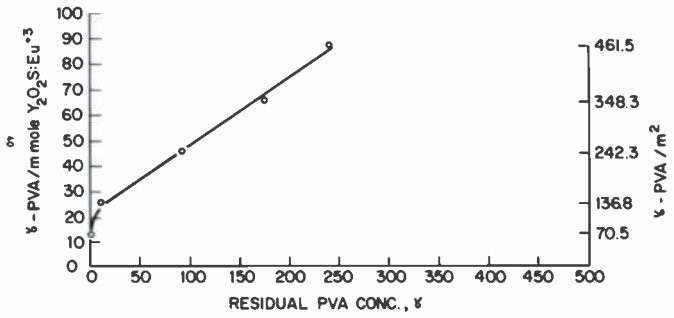

Fig. 17—Adsorption of PVA on pre-pigmented red phosphor.

density distribution occurs, with a double layer being formed, then the charge density σ can be defined as

$$\sigma = en, \qquad [12]$$

where n is the number of donor-acceptor pairs. The electron negativity series for functional groups in order of decreasing electron-donor properties is

Donor
NH_2>OH>OR>OCOR>CH_3>C_6H_3>halogens>COOR>CO>CN
Acceptor.

Usually, the most reactive group in a polymer is the *hydroxyl*.

5. Glass Substrates

It became apparent during the course of our investigations that the nature of the glass substrate was of great importance to the adher-

Table 5—Group and Total Dipole Moments[2]

Polymer	M_w	Group Dipole Moment ($\times 10^{-18}$)	Total Dipole Moment ($\times 10^{-18}$)
Vinyl acetate	86	1.75	1.75
Ethyl acetate	88	1.86	1.86
Polyvinyl acetate	24,000	1.71	28.7
	60,000	1.68	44.4
Polystyrene	12,900	0.08	0.89
	42,900	0.09	1.83

ence process. Therefore, some work was done on glasses, particularly face-plate glass.

Glass is generally thought of as an amorphous material, having a random network structure[23], pure silica being a continuous, random, three-dimensional polymer. Glasses also contain additives (impurities) that seem to reduce the melting point and viscosity, to control expansion, improve durability, and to prevent crystallization. Our FPG also contains lead for x-ray protection. The nature of the surface of a glass is controlled by the melt temperatures, volatiles lost during the melting step, volatiles lost during the hot-forming step, water vapor absorbed during forming and cooling, hydrocarbons from lubricating oils, and impurities from dies during the pressing cycle.

As discussed in previous sections, we noticed a difference in adherence between soda lime glass and faceplate glass. Since SLG could not be used in our CTV picture tube process, we concentrated on FPG.

5.1 Surface Hydroxyl (Silanol) Groups

It is well known that glass has surface hydroxyl groups.[23] The concentration of such groups can be increased by strong acids or hot strong ammonia. That such silanol groups are involved in adherence was shown by two experiments:

(1) FPG was washed in hot, concentrated ammonia, followed by the normal wash, pre-coat, slurry and developing. The adherence was found to be equivalent to the HF-etched control.

(2) FPG was etched in the normal fashion, after which surface silanol groups were removed by hexamethyldisilazine (HMDS), a well known method for removing surface hydroxyl groups.[25] In this method,

$$(CH_3)\ SiNHSi(CH_3)_3 + ROH \rightarrow ROSi(CH_3)_3, \qquad [13]$$

so that the surface hydroxyl is converted efficiently to trimethylsilyl groups.[26] Complete screens made in this fashion showed, on developing, excellent lateral coherence but no adherence to the FPG, sliding off the glass as a complete coherent screen. We find then that the wet adherence of screens is related to the glass silanols.

There is general agreement in the literature on glass that there are spectroscopic changes as glass is dehydrated and re-hydrated.

Thus, if a glass is heated above 450°C, the hydration process is not easily reversible, and the reaction is:

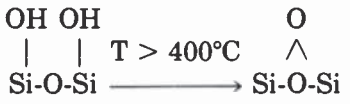

[14]

where the OH's are so-called vicinal hydroxyl groups.

Fig. 18 indicates the possible mechanisms involved in etching and pre-coating. Part (a) shows dehydrated vicinal surface hydroxyls. In part (b), the formation of silanol groups on the surface is due to etching. Part (c) shows the pre-coat PVA layer applied to the glass surface, and Part (d) indicates the oxygen-bridge bonding of pre-coat to glass surface.

This figure does not take into account the ions leached from the glass by the etchant and the interfacial results cited later in this report.

5.2 Leaching Impurities from Faceplate Glass

Faceplate glass slides, cut from the same faceplate, were leached

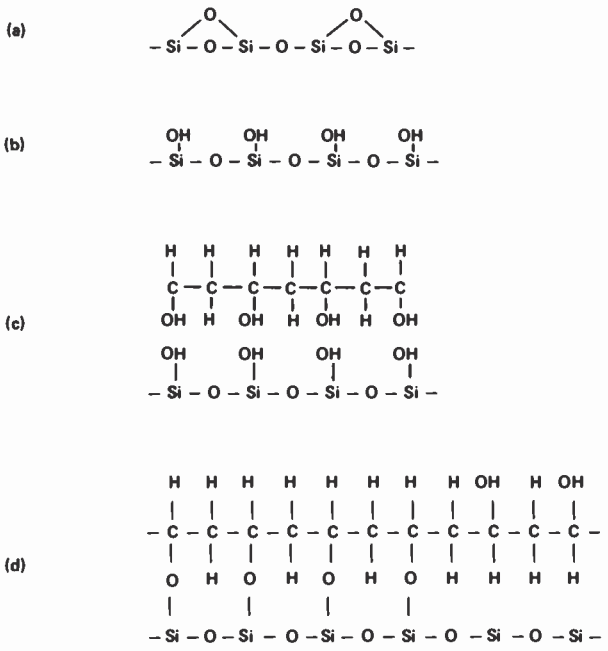

Fig. 18—Model for etching and pre-coating.

overnight in triple-distilled water in plastic containers for 0.5, 1.0, 2.0, and 4.0 hours. Runs included blanks, unwashed FPG, washed and etchd FPG, and washed, etched, and pre-coated (0.5% PVA) FPG. Samples of the water were then analyzed by optical emission spectrometry and atomic absorption.[24] The results are summarized in Table 6.

We see from Table 6 that etching serves to release a number of ions from FPG and that the concentration leached out after etching is time-dependent. The effect of the pre-coat is interesting in that pre-coating after etching results in lower leached ion concentrations in every case, even at the high (4 hour), leach time. Silicon is striking in that it is absent in the etched-precoated FPG but present in the etched FPG. It is felt that the leached ions are partially complexed by the PVA and silanols thus resulting in lower concentrations in the leach water. Relz et al.[27] have reported on the fixation of metal complexes on glasses.

Results of our experiments indicate the possibility that glass impurity ions are also involved in adherence. A possible model to explain our results at this point is shown in Fig. 19. Here, FPG has been etched to give surface silanol groups and impurity ions M. These impurity ions could be coordinated betwen glass silanols and PVA hydroxyls of the pre-coat at interface I_1 (see Fig. 2). Other impurity ions could then coordinate between hydroxyls of pre-coat PVA and of phosphor particle PVA, as in interface I_2 of Fig. 2, thus resulting in screen adherence. As will be discussed later, this is not the complete model.

5.3 Interfaces

For the exploration of interfaces (particularly I_1 and I_2) as they relate to tube processing steps in particular, we chose to investigate

Table 6—Leachable Impurities From Faceplate Glass and the Effect of Etching and Pre-Coating

FPG		Unwashed				Washed/Etched				Wash/Etch/Precoat			
Time(hrs)	Blank	0.5	1	2	4	0.5	1	2	4	0.5	1	2	4
Ba(ppm)						1	—	10	10	0.3	0.3	1	2
Sr(ppm)						12	12	60	60	10	10	12	12
Si(ppm)					2	2	2	10	6	—	—	—	—
Mg(ppm)	0.3	0.3	0.3	0.3	2	100	100	300	300	2	10	50	100
Ca(ppm)						60	60	300	300	15	15	100	100
Al(ppm)						6	6	120	120	6	6	30	30
Pb(ppm)						20	20	200	200	—	—	50	50

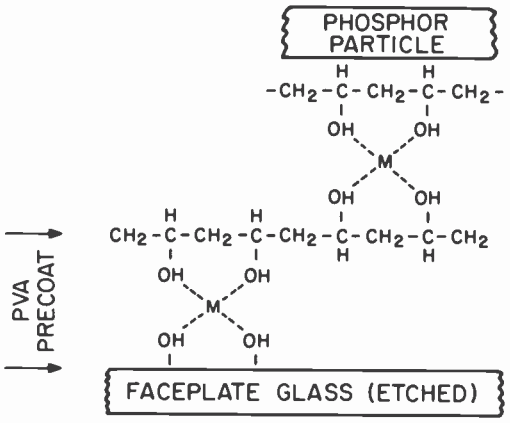

Fig. 19—Impurity ions in adherence.

contact angles. A commercial type Roué-Hart contact angle instrument was used, where advancing and receding angles could be studied as a function of tilt angle. Specially-prepared water was used as the fluid, and drops were obtained reproducibly from a calibrated Teflon microsyringe.

Contact Angles

More than 150 years ago, Young proposed treating the contact angle of a liquid on a solid as a result of the equilibrium of the drop under three surface tensions, the liquid-vapor interface (γ_{LV}), the solid-liquid interface (γ_{SV}), and the solid-vapor interface (γ_{SV}), as shown in Fig. 20. The Young equation is

$$\gamma_{SV} - \gamma_{SL} = \gamma_{LV} \cos \theta, \qquad [15]$$

where θ is the contact angle.

Since glass is a "high energy surface" (i.e., high specific surface free energy) and organics have low specific surface free energies, organics would be expected to spread on glass, as there would be a large decrease in the surface free energy of the system. We can thus consider the interfaces of Fig. 2 as a high-energy surface (FPG), on which is a low-energy surface (pre-coat), on which is another low-energy surface (phosphor PVA), which, in turn, has been deposited on a high-energy surface (phosphor).

The critical surface tension, γ_c, of PVA solid is 37 dynes cm^{-1} as reported by Scholz et al.[28], who also found γ_c to be between 40–45

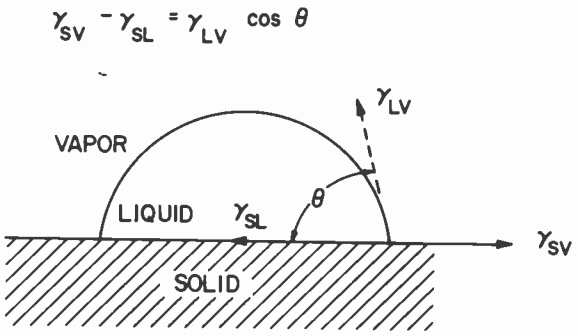

Fig. 20—Contact angles of a sessile drop.

dynes cm^{-1} for a series of hydroxyl-rich surfaces of the starch-polymer type. Spreading on low energy surfaces is caused by the lowering of the surface tension of water. Since γ_c of solid PVA is in the neighborhood of 37 dynes cm^{-1}, the solution will spread on the surface of PVA whenever a wetting agent lowers the surface tension of water below that level.

Processing and Contact Angle

Faceplate glass was taken through the steps of washing, etching, and pre-coating with 0.5% PVA 540, and contact angles were determined for each step at various tilt angles. The results were independent of tilt angle, and are shown in Fig. 21. It is seen that washed FPG has a contact angle of 30°. Etching the FPG decreased the contact angle to 10°, and pre-coating increased the contact angle to 28°. Continuing the same FPG through another wash, etch, pre-coat cycle, we see that the second wash increased the contact angle to 70°, the subsequent etch decreased the contact angle to 29°, and the following pre-coat and wash increased the contact angle again to 75°. Although only two processing cycles are shown in the figure, additional processing resulted in a repetition of these cycles. It is apparent that etching decreases the contact angle greatly, which is to be expected if the FPG surface is hydroxylated, and thus, becomes more hydrophilic. Pre-coating with PVA increases the contact angle, making the glass less hydrophilic.

The first three steps of Fig. 21 correspond to the initial processing for the first phosphor in a CTV kinescope. This first phosphor slurry is applied, dried, exposed, and developed. At this point, however,

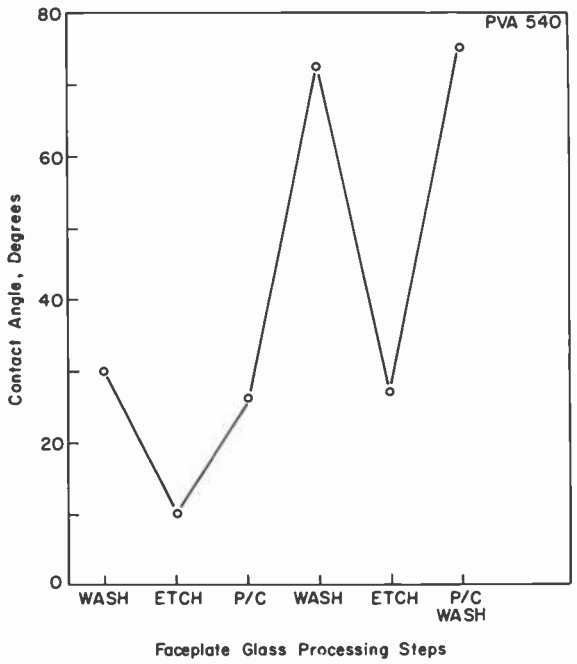

Fig. 21—Contact angle vs processing step.

the FPG contact angle increases toward hydrophobicity (before the second phosphor slurry is applied). What happens to adherence? We investigated this by making blue screens and measuring the adherences for FPG treated to have $\theta = 30°$ and $\theta = 70°$. We found adherence = 220 for $\theta = 30°$, and 156 for $\theta = 70°$, or a ratio of 1.41. The work of adherence on a surface, W_a, is given by

$$W_a = \gamma_L (1 + \cos\theta) \qquad [16]$$

γ_L was measured with a DuNouy tensiometer; $W_a^{30°}$ was calculated as 125.1 and $W_a^{70°}$ as 90.1, a ratio of 1.39. It would appear therefore that adherence of our phosphor screens is related to the work of adherence on the surface, which would therefore call for the smallest contact angle, which we obtain by etching the FPG.

When we wash the pre-coat layer, θ increases to 70° instead of decreasing to 10°, as it did after the first etching. This is interpretable as further evidence that a hydrophobic layer exists in interface 1, quite possibly contiguous to the glass as shown in Fig. 22. It may be formed by a coordinated metal-ion-PVA reaction, and there is

unreacted PVA on its surface. Washing the surface will remove interface I_{1B} (Fig. 22), thereby exposing interface I_{1A}. Subsequent etching might remove most, but not all, of 1A, thereby decreasing θ, but not to the θ value of the original etched surface. It is of interest that recent work has appeared on metal in complexes with PVA.[29] In terms of adhesion, partly-hydrolized PVA has been described for highly hydrophobic polymer surfaces.[30]

6. Adherence as a Function of Processing Steps

Our technique of measuring adherence by jet-impingement 3 × 3 inch sections of phosphor screens on FPG enables us to examine the variation in adherence during the processing procedure.

The adherence of dried pre-coat was measured by precoating a slide, drying it, and jet-impinging. The hole made by the jet is rendered visible by treating the slide with methylene-blue-dye dissolved in methanol. This dye stains the PVA so that the hole is easily measured and the adherence calculated. Similar adherence measurements were made after the slurry was applied and dried, after exposure, and after development. The results are shown in Fig. 23. We see that pre-coat adherence is very low, and dried slurry adherence is only about 35% higher. Exposing the screen increases the adherence by a factor of fifty, but the developing step reduces it by a factor of three. Soda lime glass, while showing identical adherence for pre-coat and slurry, shows better adherence than FPG after exposure and after development.

These results indicate the importance of interfaces I_3 and I_4 in the adherence procedure. For these cases, the dichromate sensitization step becomes important in cross-linking the PVA and thus bonding the phosphor particles. Grimm et al.[30] have discussed the photochemical reactions in a dichromated resist, and this aspect will

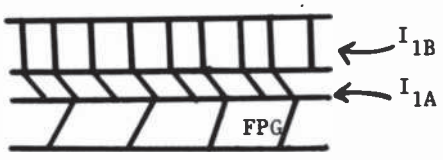

Fig. 22—Coordinated metal-ion interface.

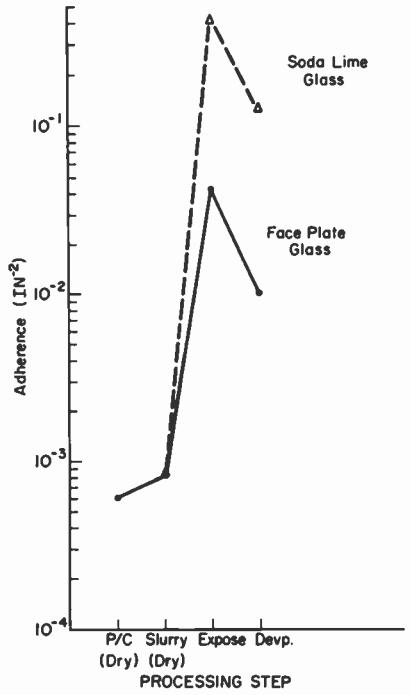

Fig. 23—Adherence vs processing steps.

not be reviewed here. From our point of view, the sensitized PVA-phosphor slurry provides for inter-particle bonding, the first particles of which form I_2 (Fig. 2).

7. Contact Characteristics of Model Slurries

The contact properties of model slurries, prepared with PVA540, were investigated since these properties are important in commercial tube production. Tube simulation studies were carried out using FPG, which was washed, etched, pre-coated with PVA540, and dried.* Contact angles were determined on this surface for water and for pre-pigmented blue phosphor model slurry (surface tension = 40.2 dynes cm^{-1}), which corresponds to the deposition of the first phosphor. This FPG substrate was then water-washed, corre-

* The abbreviated notation developed during this work would be: FPG/W/E/PC540/D//.

Table 7—Blue Model Slurry Contact Properties

Processing Steps	Blue Slurry		H_2O	
	θ	W_A	θ	W_A
FPG/W/E/PC/D//	58° ± 3°	62	37° ± 3°	121
FPG/W/E/PC/D/W/D//	39° ± 3°	72	66° ± 3°	94

sponding to the developing step, and dried, giving a total history of FPG/W/E/PC540/D/W/D//, and contact angles were again determined for water and for the blue slurry, which now corresponded to the *second* phosphor layer.

Consistent with the results shown in Fig. 21, the surface seen by the second layer of blue phosphor is more hydrophobic than that seen by the first layer of phosphor, so that the energy of wetting of the blue phosphor is different, depending on whether it is deposited as a first layer or as a second layer. Similarly, W_A, the work needed to remove a film, increases as the surface becomes more hydrophobic. These results are summarized in Table 7. Interestingly, the third phosphor deposition "sees" a more hydrophilic surface, perhaps due to build-up of PVA on the surface.

It would appear from these results that the more hydrophilic a surface, the more "organophobic"; and the more hydrophobic the surface, the more "organophilic" as applying to the model phosphor slurry.

Having investigated the contact angle of (blue) slurry, we examined separately deposition of the resist component (PVA540) on pre-coats of PVA540 and PVA165. A comparison of the results shown in Table 8 with Table 7 shows (a) PVA540 resist acts in an identical fashion for contact angle, with PVA540 or PVA165 precoats and (b) that the contact angle is determined primarily by the resist portion of the slurry. The surface tension of the resist was measured as 39 dynes cm^{-1}.

Results shown in Table 7 indicate that the PVA pre-coated surface is hydrophilic, and organophobic. When the PVA pre-coated

Table 8—Contact Angles of PVA540 Resist on PVA540 and PVA165 Pre-coats

Processing Step	PVA540PC θ	PVA165PC θ
FPG/W/D//	46° ± 3°	42° ± 3°
FPG/W/E/D//	40° ± 3°	45° ± 3°
FPG/W/E/PC/D//	59° ± 3°	61° ± 3°
FPG/W/E/PC/D/W/D//	45° ± 3°	42° ± 3°

surface is washed, the new surface becomes more hydrophobic and more organophilic to the blue slurry. While this might be due to acetyl groups on the PVA540 pre-coat, the results in Table 8 for PVA540 and for PVA165 show that this is not the case.

What would be the effect of changing the type of PVA pre-coat on the contact angle of water? For these experiments, PVA165, D.H. = 99.7%, was used as the pre-coat. Results, including the previous PVA540 pre-coat for comparison purposes, are given in Table 9.

It is interesting to note that for PVA165 the ratio of W_A is 0.9, and the adherence ratio is 1. Similarly, for PVA540, the W_A ratio is 1.3 and the adherence ratio is 1.4.

8. Other Effects

FPG Surface Additives

Since the etching step appears to have two functions, silanol formation and release of impurity ions, experiments were performed where the FPG surface was exposed to a given ion and dried prior to pre-coating, thus eliminating the etch step. Fair adherences were obtained in this manner with an apparent correlation between adherence and the solubility product of the metal-ion-sulfide. That the green (sulfide) phosphor was necessary for adherence was established by applying resist (no phosphor) to the surface-treated unetched FPG. No adherence was obtained. With green slurry, adherence appeared. For the ions tried, the adherence order was: copper (S.P. of the sulfide 10^{-47}) best, followed by cadmium (S.P. 10^{-29}) and zinc (S.P. 10^{-23}).

Pre-Coat Additives

We also investigated the addition of inorganic ions to the PVA pre-coat to provide a highly cross-linkable region at interface I_1, the critical interface for adherence. Y^{3+} was used as the additive, since previous work here[31] had shown it to have a cross-linking effect.

Table 9—PVA165 and PVA540 Pre-coats

	PVA165			PVA540		
	θ_{H_2O}	W_A	ADH.	$H_2^{\circ}O$	W_A	ADH.
FPG/W/E/PC/DRY//	52°	108	115	37°	121	222
FPG/W/E/PC/DRY/W/D//	40	119	115	66	94	156

Experimental results did indeed show an increased adherence for screens prepared with yttrium-doped pre-coats. Fig. 24 shows the yttrium-effect on the adherence of our green model slurry, the optimum being at about 50 micrograms of yttrium. However, this effect was absent with slurry containing triethyleneglycol because the yttrium evidently complexed with the triethyleneglycol in the slurry, thereby becoming unavailable for crosslinking at the interface.

Slurry Additives

Triethyleneglycol (TEG) was investigated as an additive to our green model slurry. Using our standard procedure, namely, FPG/W/E/PC/D//, we found that the adherence increased monotonically with increasing TEG, as shown in Fig. 25. It is believed that this particular effect can be accounted for by the increase in sensitivity found with the addition of TEG. Over the range of TEG/PVA covered in our experiments, Fonger[32] has reported a monotonic decrease in threshold, τ, also shown in Fig. 25. This increase in sensitivity produces an increase in adherence for a constant time (and intensity) of exposure.

Aging Effects in Slurry

During the course of these investigations, it was observed that

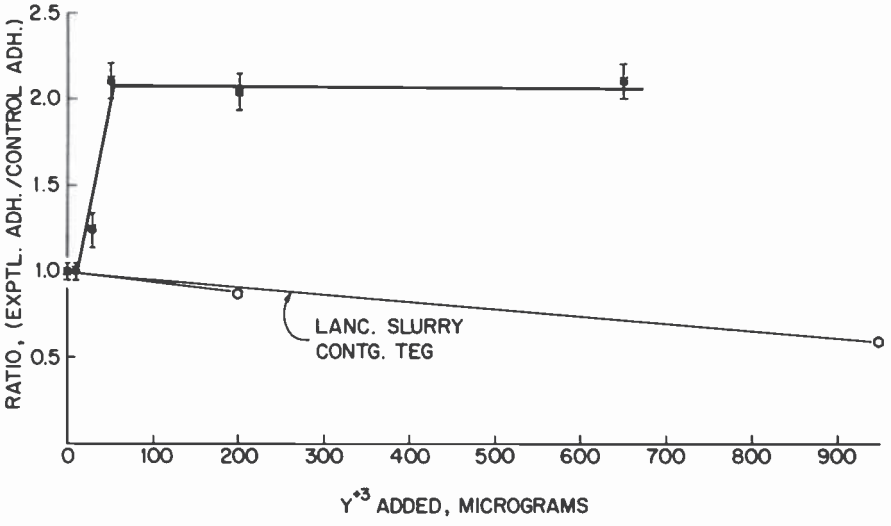

Fig. 24—Adherence vs pre-coat Y^{+3} concentration.

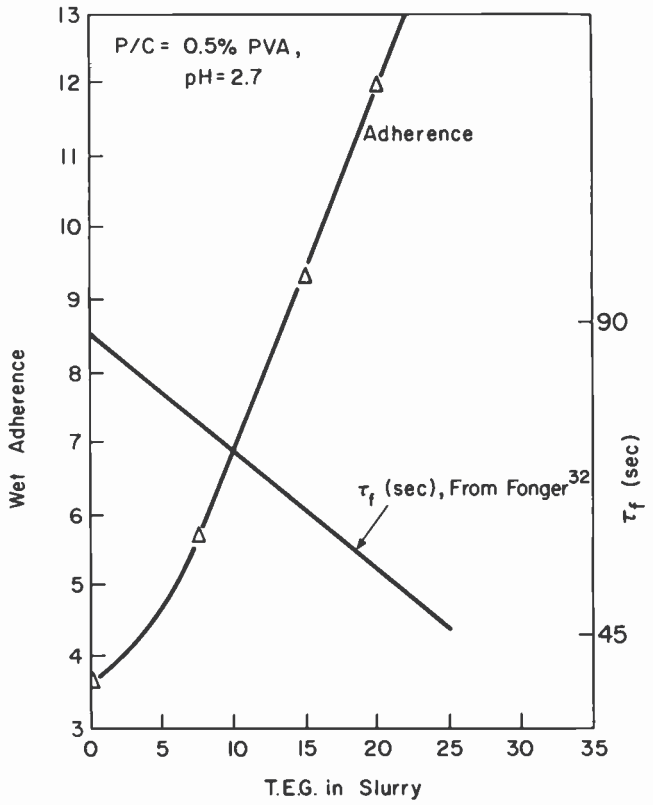

Fig. 25—Effect of TEG on adherence.

aging effects were taking place, i.e., adherence appeared to improve as our green slurry aged. This was examined in some detail, and the results are shown in Fig. 26 where we see that maximum wet adherence occurred after about six days aging. Such effects might be related to cluster growth in the slurry to an optimum size. Caution must be observed in investigating aging effects, since other parameters may be operative. For example, aging in blue slurry showed a decrease in adherence that could be correlated with the effect of Mg^{++} ions (used in the phosphor) on the hydroxyl ion concentration. This is shown in Fig. 27.

Plasma-Treated Pre-Coats

Plasma-treating the pre-coat could effect cross-linking. It might also effect the aldehyde and ketone concentrations in the PVA and the

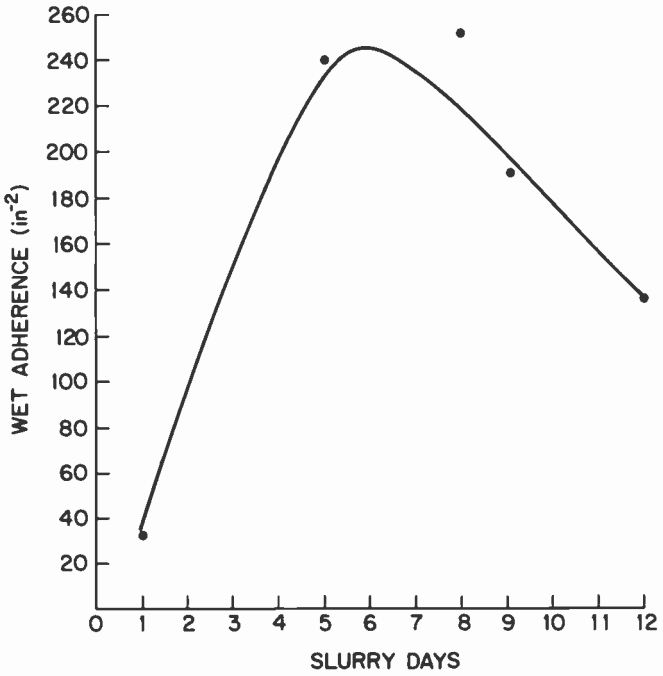

Fig. 26—Adherence vs aging for green slurry.

proportion of high-molecular-weight polymer. Exploratory runs were made[33] on PVA-precoated faceplate glass. Results are summarized in Table 10.

In summary, a one-minute treatment with Ar or Ar + H_2 plasma had no effect. However, extending the plasma time to ten minutes resulted in a large decrease in adherence for Ar-plasma, but in an increase for samples treated in Ar + H_2 plasma.

Pinning

The availability of hydroxyls for bonding in a polymer molecule is of leading importance. If we consider the case of an ideal, uncoiled, linear PVA, we note that the hydroxyl unit repeats for every alternate carbon on the backbone. If we now consider such a PVA on an idealized glass surface (i.e., with a silanol for every surface silicon), we would have a matching hydroxyl ratio of PVA/glass of 1:2, or $N_m \approx 0.5$. We can thus consider, for this case, that half the silanols are "pinned".

Now consider more rigid polymers having hydroxyl groups, such

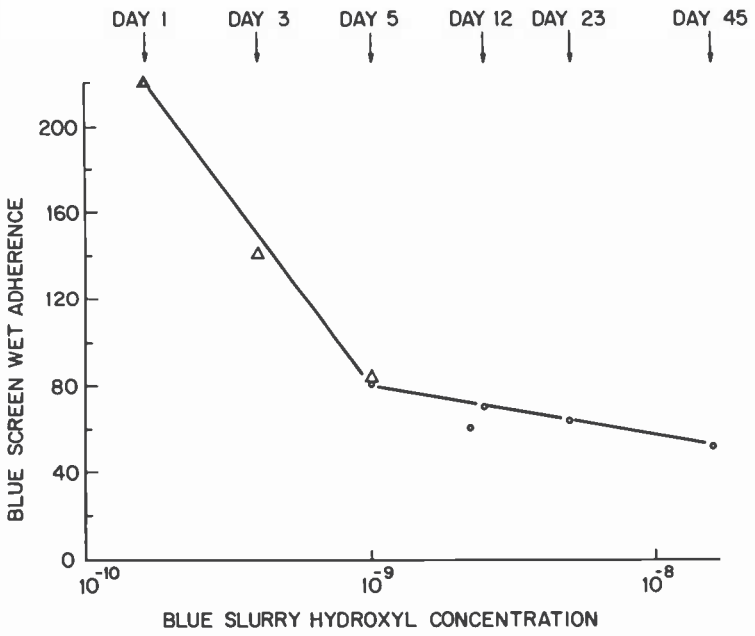

Fig. 27—Adherence vs aging for blue slurry.

as hydroxyethylcellulose (HEC) and hydroxypropylcellulose (HPC). HEC has three hydroxy groups available per anhydroglucose unit of the cellulose. Due to steric considerations, two possibilities exist for "pinning", one with $N_m \approx 0.2$ and another with $N_m \approx 0.1$. Using HEC as a precoat resulted in a screen adherence factor about six times worse than with PVA. It is interesting to compare that value to the ratio N_m^{PVA}/N_m^{HEC} which is 2.5 for one steric case and 5.0 for the second.

For the HPC case, steric hindrance and hydrogen-bonding considerations show that essentially none of the hydroxyls would be available for silanol "pinning", and our adherence experiments show no adherence when HPC is used as a precoat material.

Table 10—Plasma Treatment Effects on PVA-Precoated FPG

Plasma	Time (min)	Adherence Ratio*
Ar	1	1.00
Ar	10	0.32
Ar + H_2	1	1.00
Ar + H_2	10	1.40

* Ratio of plasma-treated sample adherence to non-treated sample.

The above data, together with our work on adherence as a function of hydroxyl content, lead to important considerations: (1) hydroxyaliphatics will yield higher "pinning" ratios than hydroxyaromatics; (2) poly(vinyl alcohol), with a "pinning" ratio of about 0.5 is a good precoat; (3) new precoats with pinning ratios greater than 0.5 should be explored.

9. Discussion

The wet adherence of phosphor screens to faceplate glass is a highly complex phenomenon involving many parameters, only a few of which have been described in this paper. The complexity is increased by the fact that many of the parameters involving adherence are not isolated but operate as interlinked systems.

Our investigations involved mainly interfaces and their effect on adherence as changes were made. Thus, we have investigated the phenomenon of etching and its effect of the glass surface. Our findings that etching with NH_4HF (or with NaOH) probably forms surface silanol groups, as well as releasing impurities from the glass, link well with the application of a PVA pre-coat whose hydroxyls can (1) react with the silanols to bond the precoat to the faceplate glass, and (2) form coordination compounds with the impurities. Other unreacted pre-coat hydroxyls react with phosphor particle PVA to bond such particles to the precoat. Interfacial chemical bonding has been discussed recently by Runge[34] for the case of glass-polybutadiene joints. The experiments we report on etchless adherence by impurity addition are of interest, particularly as adherence appeared to be a function of the solubility product of the metal sulfide. This would indicate the possibility of diffusion of the metal ion through PVA interfaces to bond with surface sulfide of the phosphor. VanOoij[35] has reported on the mechanism of rubber-to-brass adhesion which he finds due to a thin film of cuprous sulfide formed on the brass surface, with sulfur atoms being transferred to rubber molecules, thus giving interaction adhesion. Our work has indicated an optimum pre-coat film thickness for adherence and VanOoij also reports film thickness effects in his work. It is possible that our precoat optimum thickness is the limiting thickness for diffusion of metal ions. Obviously, much more work remains to be done, utilizing such techniques as ESCA, XPS, STEM, and FTIR to further characterize the surfaces and interfaces.

We have explored the effects of differences in degree of hydrolysis and degree of polymerization of the PVA and have shown the usefulness of the concept of hydrodynamic parameters to characterize

PVA. Zeta-potentials were obtained for portions of our system, and contact angles have established that successive layers of phosphor slurry see different surface conditions. Contact angle changes as a function of processing step for faceplate glass have been investigated, and the results indicated that wet adherence is dependent on contact angle and can be correlated with surface energy. The problem of crosscontamination is undoubtedly also related to surface effects of the initial and contaminating phosphors, as previous work has shown.[36] This problem has not been treated in the present work and remains to be explored in depth, particularly as it relates to surface coatings. A recent paper[37] has examined some changes in adhesion forces during picture-tube production.

The roles of double layer and of polymer inter-diffusion in adherence should be examined. At interface I_2, we have pre-coat PVA interfacing phosphor (slurry) PVA. If this is treated as the case of two identical polymers in contact, we would not expect much adherence from the doublelayer donor-acceptor aspect. Thermal motion of the molecules of the chain could lead, at the extreme case, to a mixed layer of complete mutual intersolubility. Exposing the phosphor slurry acts to cross-link the PVA, so that the phosphor PVA and the pre-coat PVA are no longer identical. However, mobility of some of the segments (although the chains are immobile translationally) can give a limited inter-diffusion, which should give a large increase in adherence. Josefowitz and Mark[38] have discussed the role of chain-segment diffusion as applied to polymer self-adherence. Interface I_2 can thus be pictured as consisting of a sensitized exposed PVA in contact with a thin PVA coating that contains ions leached from the underlying faceplate glass. Such a model for interface I_2 would provide for a limited inter-diffused region for greater adherence. The role of the exposure then would include both providing for the phosphor particle-to-particle adherence through mutual cross-linking and providing for segment interdiffusion with the PVA pre-coat. It is of interest that Deryagin[2] gives the width of the interface diffusional zone necessary for the contact of several pairs of polymers as ranging from 6×10^{-2} mm for paraffin/SKN to 10^{-3} mm for SKB/chlorinated PVC, with an average of about 10^{-3} mm. This compares to about 10^{-4} mm for the optimum pre-coat thickness we found for PVA pre-coat on faceplate glass. In addition, since we are interested in maximizing the inter-polymer donor-acceptor pair population, it might be well to consider a double-layer system with dissimilar polymers for precoat and for phosphor slurry.

10. Conclusions

The adherence of phosphor screens to faceplate glass substrates is a complex phenomenon involving several interfaces and effects including the glass, the PVA, the pre-coat, and sensitization. A new method for determining adherence was evolved as part of this investigation. The effects of etching have been shown to involve silanol groups and release of impurities from the glass substrate. These, in turn, operate on the pre-coat, which has an optimum thickness and serves as an "impedance-matching" layer, binding both to the substrate and to the initial layer of phosphor particles, these interfaces being most important in adherence.

Characterization of the PVA can be carried out by determining the hydrodynamic parameters which relate to adherence. Similarly, interfacial properties can be characterized by the contact angle of the surfaces to water, resist or slurry. It has been found that phosphor slurries see different surfaces as a faceplate is screened in the shadow-mask process. The largest deviation of surface from best adherence takes place with the deposition of the second phosphor. Data on contact angle versus the screen processing step has been obtained, and adherence has been shown to be correlatable with the energy necessary to remove a screen from a surface.

An examination of the role of zeta-potentials, combined with PVA adsorption studies, indicate their possible initial importance in the adherence process, particularly with the addition of certain additives. The role of triethyleneglycol in promoting adherence was confirmed, and attributed to its effect in decreasing the sensitivity threshold.

Finally, models of etched, precoated, screened substrates were evolved.

11. Acknowledgments

The authors are grateful to the following individuals for their aid in conversations, equipment or advice: A. E. Hardy, S. A. Harper, M. R. Royce, and S. Trond of RCA Lancaster; P. N. Yocom, Y. Arie, S. Berkman, P. Datta, K. B. Kilichowski, M. Labib, A. W. Levine, H. H. Whitaker, and P. J. Zanzucchi of RCA Laboratories.

References:

[1] K. L. Mittal, Extended Abstracts, Electrochemical Society, Vol. 81-1, May 10–15, 1981, Minneapolis, Minnesota, p. 327.

[2] B. V. Deryagin, N. A. Kratova, and V. P. Smilga, *Adhesion of Solids,* Consultants Bureau (trans.), 1978.
[3] A. D. Zimon, *Adhesion of Dust and Powder,* Consult. Bur., NY, 1982.
[4] W. Fonger, private communication.
[5] M. Matsumoto and Y. Ohyanagi, *Kobunshi Kugaku* **17,** 17 (1960).
[6] H. G. Elias, *Makromol. Chem.* **54,** 78 (1962).
[7] I. Sakurada, *J. Soc. Chem. Ind.* (Japan) **47,** 137 (1944).
[8] P. J. Flory and T. G. Fox, *J. Am. Chem. Soc.* **73,** 1904 (1951).
[9] L. K. Koopal and J. Lyklema, *Faraday Disc. Chem. Soc.* **59,** 230 (1975).
[10] J. G. Pritchard, *Poly(Vinyl Alcohol),* Gordon and Breach, London, 1970.
[11] E. N. Rostovskii and L. E. De-Millo, *Zh. Prikl. Khim.* **36,** 1821 (1963).
[12] G. Natta et al., *J. Am. Chem. Soc.* **77,** 1708 (1955).
[13] C. A. Finch, *Polyvinyl Alcohol,* Wiley, London (1973), Chapt. 10.
[14] C. Y. Liang and F. G. Pearson, *J. Polym. Sci.* **25,** 303 (1959).
[15] J. F. Kenny and G. W. Willcockson, *J. Polym. Sci.* **A-1, 4,** 690 (1966).
[16] S. A. Harper, private communication.
[17] H. D. Wilcox, U.S. Patent 3,940,508, issued 2/24/76.
[18] G. Auth, private communication.
[19] M. M. Zwick, *J. Appl. Polym. Sci.* **9,** 2393 (1965).
[20] E. D. Yakhnin et al., *Makromal. Gran. Razdela Faz,* 212–217 (1971); C. A. **79,** 149805e (1973).
[21] T. F. Tadros, *ACS Symp. Colloid Dispers.,* 173 (1975).
[22] M. J. Garvey, T. F. Tadros and B. Vincent, *J. Coll. Interface Sci.* **55** (2), 440 (1976).
[23] M. L. Hair and A. M. Filbert, *Surface Chemistry of Glass,* R/D, 1969.
[24] H. L. Whitaker, private communication.
[25] See, for example, R. J. DePasquale, *Amer. Lab.,* pp. 34–39, June 1973.
[26] J. Bohemen et al., *J. Chem. Soc.* 2444 (1960).
[27] J. Relz, K. Unverferth and K. Schwetlick, *Z. Chem.* **14** (9), 370 (1974).
[28] J. T. Scholz et al., *J. Phys. Chem.* **62,** 1227 (1958).
[29] J. Frances, M. Ishaq, and M. Tatsui, *Organo Trans. Met. Chem. Jap.,* pp. 57–64 (1975).
[30] L. Grimm, K.-J. Hilke, and E. Scharrer, *J. Electro. Chem. Soc.* **130,** 1767 (1983).
[31] S. Larach and J. E. McGowan, unpublished data.
[32] W. H. Fonger, private communication.
[33] Y. Arie, private communication.
[34] M. L. Runge and P. Dreyfuss, *J. Polym. Sci.* **17,** 1067 (1979).
[35] W. J. van Ooij, *Rubber Chem. and Tech.* **51,** 52 (March-April 1978).
[36] S. Larach and J. E. McGowan, unpublished work.
[37] E. Scharrer, L. Grimm, H. Mayatepek, and W. Ritsert, *J. Electro. Chem. Soc.* **130,** 1762 (1983).
[38] D. Josefowitz and H. Mark, *India Rubber World* **106,** 33 (1942).